Low-power OTA-C Based Tuneable Fractional Order Filters

Ibrahim Ethem Sacu[1], Mustafa Alci[2]

[1]Institute of Natural and Applied Sciences, Erciyes University, Kayseri, Turkey
[2]Department of Electrical and Electronics Engineering, Erciyes University, Kayseri, Turkey

Abstract: In this study, a low-voltage low-power, simple operational transconductance amplifier (OTA) based fractional order low-pass and high-pass filters of order (n+α) are designed and simulated with CADENCE-PSPICE where 0<α<1 and n≥1. The employed transconductance amplifier operates at ±0.75 V. To simulate designed filters, 0.35 μm TSMC CMOS technology parameters are used. The simulation results verify theoretical statements. The power dissipations of simulated low-pass filters of orders 1.3, 1.5, 2.3 and 2.5 are 14.6 nW, 13 nW, 17 nW and 15.3 nW, respectively. For the same filter orders, the corresponding dissipation values of high-pass filters are respectively 45.2 nW, 42.7 nW, 47.5 nW and 45 nW. In addition to the low-power low-voltage operation, another significant advantage of the proposed circuit topologies is that the OTA based low-pass and high-pass topologies provide electronic tuning capability of the orders and frequency responses of the filters without any structural change on these topologies. Therefore, same circuit topology can be used for the different orders of the same filter by just changing the biasing currents of the used OTAs. Additionally, OTA-C based filters offer usage of the grounded capacitors as well as resistorless realization.

Keywords: Fractional filter; fractional circuit; low power

Nastavljiv filter frakcijskega reda nizkih moči na osnovi OTA-C

Izvleček: Članek predstavlja nizko in visoko pasovne filtre nizkih napetost in majhne moči na osnovi transkonduktančnega operacijskega ojačevalnika (OTC). Filtri reda (n+α) so načrtani in simulirani v CADNECE_PSPICE okolju, pri čemer je 0<α<1 in n≥1. Transkonduktančni ojačevalnik deluje pri napetosti ±0.75 V. Filtri so simulirani v 0.35 μm TSMC CMOS tehnologiji. Poraba moči simuliranih nizkopasovnih filtrov reda 1.3, 1.5, 2.3 in 2.5 so 14.6 nW, 13 nW, 17 nW in 15.3 nW. Visokopasovni filtri enakih redov porabijo 45.2 nW, 42.7 nW, 47.5 nW in 45 nW moči. Nizko napetostno delovanje pri nizki porabi moči omogoča možnost elektronske nastavitve reda filtra brez spreminjanja topologije. Ista topologija tako omogoča izvedbo filtra različnega reda le s spreminjanjem mirovnega toka OTA. Filti na osnovi OTA-C omogočajo ozemljitev kondenzatorjev in izvedb o brez uporabe uporov.

Ključne besede: frakcijski filter; frakcijsko vezje; nizka moč

* Corresponding Author's e-mail: malci@ erciyes.edu.tr

1 Introduction

Fractional calculus is a branch of mathematics that considers differential equations of arbitrary order in contrast to classical calculus. It eliminates the requirement that the order of differential equations has to be integer. Therefore, it generalizes conventional differential and integral equations and helps the modelling of the real world phenomena better [1, 2]. Fractional calculus has found applications in engineering, biology, control, viscoelasticity, electromagnetism, diffusion theory etc. [3]. By applying fractional calculus to electronics, sinusoidal oscillators, multi-vibrator circuits, phase locked loops, analogue fractional order controllers, differentiators-integrators and fractional order filters have emerged [3-23].

In the literature, several definitions of fractional derivatives have been proposed. One of them is the Riemann and Liouville fractional derivative, which is given as

$$\frac{d^{\alpha}}{dt^{\alpha}} f(t) \equiv D^{\alpha} f(t) = \frac{1}{\Gamma(1-\alpha)} \frac{d}{dt} \int_0^t \frac{f(\tau)d\tau}{(t-\tau)^{\alpha}} \qquad (1)$$

where Γ(.) is the Gamma function and fractional order α is 0<α≤1 [4]. Applying the Laplace transform to (1) with zero initial conditions yields

$$L\left\{ {}_0^C D_t^\alpha (t) \right\} = s^\alpha F(s) \tag{2}$$

where s^α is called the fractional Laplacian operator [14].

Even though a non-integer order filter is usually required based on the specifications of applications, current practice rounds off the filter order to the nearest integer. Therefore, the filters used today are integer orders. However, this approach limits the freedom of design. Fortunately, introducing fractional calculus into filter design removes this limitation and presents some advantages. The main advantage is that it enables the stepping attenuation of the fractional filter that is −20×(n+α) dB/dec or −6×(n+α) dB/oct [2].

In all of the designs of fractional order filters, the fractional Laplacian operator s^α has been used, due to the fact that transfer functions can be designed easily. However, a standard two-terminal component, which meets the fractional Laplacian operator, has not as yet been produced. Therefore, different methods have been proposed for approximating the fractional Laplacian operator. By means of these methods, integer order transfer functions are achieved [16]. In previous studies on fractional filters, namely fractional domain first order filters and second order filters, researchers mostly prefer to emulate s^α via R-C networks [3, 13, 17]. Instead of following this procedure, in this study substitution of the integer order approximation function into s^α is preferred and then the final transfer function is used for implementation.

In this paper, by using the (1+α) order transfer function provided by [3], OTA-C based fractional step approximated Butterworth filter circuits of order (n+α) are designed and simulated. The aim of this study is not designing a new OTA active element or improving of OTA performance metrics. On the contrary, the target of this study is exploiting of OTAs presented features for designing fractional order filters.

2 Design steps of the fractional order filters

In this section, general design equations for the approximated fractional order low-pass and high-pass filters of orders of (1+α) and (n+α) are derived and given in order.

2.1 The Approximated fractional Butterworth low-pass filters of order (1+α)

The transfer function of the low-pass filter of order (1+α) was firstly introduced by [17] but it has an undesired peak in the pass-band. The modified version of the transfer function of the approximated fractional order Butterworth low-pass step filter was proposed by Freeborn et al. as [3]

$$H_{1+\alpha}^{FLP} = \frac{c_1}{s^\alpha (s + c_2) + c_3} \tag{3}$$

where c_1, c_2 and c_3 are coefficients which are determined by nonlinear curve fitting to achieve Butterworth characteristics in the frequency response. As mentioned above, there is no commercially available electronic device to make the characteristics of the fractional Laplacian operator s^α available. A solution of this problem is the using integer order circuits. Therefore, approximation methods like Carlson, Oustaloup, Matsuda, Continued Fraction Expansion (CFE) and the Charef method can be used. However, the resulting approximation functions are only valid in a limited frequency band. As the order of the approximation function increases, the accuracy as well as frequency band increase. Also, it demands more in terms of the hardware and power. Therefore, there is a trade-off between accuracy and cost in hardware. Among these methods, the CFE method was preferred in this study from the circuit complexity point of view [9, 24].

According to the CFE method, the second order approximation function of s^α is defined as [9]

$$s^\alpha \cong \frac{(\alpha^2 + 3\alpha + 2)s^2 + (8 - 2\alpha^2)s + (\alpha^2 - 3\alpha + 2)}{(\alpha^2 - 3\alpha + 2)s^2 + (8 - 2\alpha^2)s + (\alpha^2 + 3\alpha + 2)} \tag{4}$$

Substituting (4) into (3), the following integer order transfer function is derived as

$$H_{1+\alpha}^{FLPF}(s) \cong \frac{c_1}{m_0} \frac{(m_2 s^2 + m_1 s + m_0)}{s^3 + k_0 s^2 + k_1 s + k_2} \tag{5}$$

The expressions for m_0, m_1, m_2 and k_0, k_1, k_2 are found as

$$
\begin{aligned}
m_0 &= \alpha^2 + 3\alpha + 2 \\
m_1 &= 8 - 2\alpha^2 \\
m_2 &= \alpha^2 - 3\alpha + 2 \\
k_0 &= (m_1 + m_0 c_2 + m_2 c_3)/m_0 \\
k_1 &= (m_1(c_2 + c_3) + m_2)/m_0 \\
k_2 &= (m_0 c_3 + m_2 c_2)/m_0
\end{aligned}
\tag{6}
$$

The values of c_1, c_2 and c_3 are determined by curve fitting by minimizing the cumulative pass-band error between responses of $H_1^{BWLPF}(s)$ and $H_{1+\alpha}^{FLPF}(s)$, where $H_1^{BWLPF}(s)$ and $H_{1+\alpha}^{FLPF}(s)$ are the 1st order and the $(1+\alpha)$ order fractional Butterworth filter responses, respectively.

Before realizing the fractional order transfer functions, the stability of the fractional order transfer functions must be determined. To achieve that, the s to w domain transformation which requires that $w=s^{1/m}$ is selected. In this transformation, it is assumed that all of the fractional orders can be expressed as $\alpha_i=k_i/m$ ($i=1,2,3,\ldots$) where m is the common factor. The stability condition of this method is that all of the pole angles $|\theta_{wi}|$ have to be greater than $\pi/(2 \times m)$. Detailed information and examples about stability can be found in [25]. According to the s to w domain transformation, for $\alpha=0.3$ and $\alpha=0.5$, the following characteristic equations from (3) are obtained as

$$w^{13} + 0.477w^3 + 0.8 \quad (\alpha = 0.3) \tag{7a}$$

$$w^{15} + 0.68w^5 + 0.859 \quad (\alpha = 0.5) \tag{7b}$$

where $s=w^{1/10}$. For both of the characteristic equations, the stability condition is that the pole angles $|\theta_{wi}|$ ($i=1,2,3,\ldots$) have to be greater than $\pi/(2 \times 10)$. The minimum pole angles for (7a) and (7b) are calculated as $|15.1671°|$ and $|14.1656°|$ respectively, which satisfy the stability condition being greater than $9°$.

To realize the integer order transfer function of (5), a block diagram (BD) of the inverse follow the leader feedback (IFLF) with the input distribution form can be used. The function of (5) can also be achieved by cascading of the first order transfer function of an integrator and second order transfer function of the single amplifier biquad (SAB) or the multiple amplifier biquad (MAB). But this way does not provide electronic tuning capability, at the same time it increases design complexity and power consumption. Thus, the IFLF form design is preferred. The BD diagram of the fractional low-pass filter is shown in Fig.1 where G_i ($i=0,1,2$) corresponds to the scaled version of corresponding output quantity. The transfer function of this topology is expressed as

$$H(s) = \frac{\dfrac{G_2}{T_1}s^2 + \dfrac{G_1}{T_1 T_2}s + \dfrac{G_0}{T_1 T_2 T_3}}{s^3 + \dfrac{1}{T_1}s^2 + \dfrac{1}{T_1 T_2}s + \dfrac{1}{T_1 T_2 T_3}} \tag{8}$$

where G_0, G_1, G_2 and T_1, T_2, T_3 are gains and time constants, respectively. By equating (5) with (8), it can be obtained that

$$G_2 = \frac{c_1 m_2}{k_0 m_0}, G_1 = \frac{c_1 m_1}{k_1 m_0}, G_0 = \frac{c_1}{k_2}$$

$$T_1 = \frac{1}{k_0}, T_2 = \frac{k_0}{k_1}, T_3 = \frac{k_1}{k_2} \tag{9}$$

At the circuit realization, expressions in (9) will be utilized to determine the bias currents of OTAs in the filter.
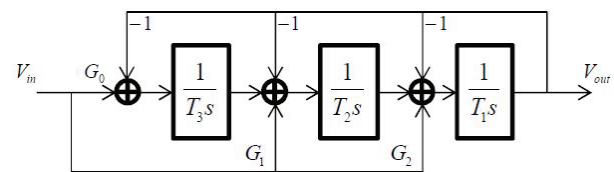

Figure 1: The BD diagram of the approximated Butterworth low-pass fractional order filter

2.2 The Approximated fractional Butterworth high-pass filters of order (1+α)

The transfer function of the fractional high-pass filters of order $(1+\alpha)$ can be obtained by replacing s with $1/s$ in (3). By performing this transformation and same steps in the Section 2.1, the following transfer function is derived as

$$H_{1+\alpha}^{FHPF}(s) \cong \frac{(c_1/c_3)}{k_0} \frac{(m_0 s^3 + m_1 s^2 + m_2 s)}{s^3 + \dfrac{k_1}{k_0}s^2 + \dfrac{k_2}{k_0}s + \dfrac{k_3}{k_0}} \tag{10}$$

The expressions for m_0, m_1, m_2 are same as those in (6), but the expressions k_0, k_1, k_3 and k_4 are found as

$$\begin{aligned} k_0 &= m_0 + (m_2 c_2 / c_3) \\ k_1 &= m_1 + ((m_1 c_2 + m_2)/c_3) \\ k_2 &= m_2 + ((m_0 c_2 + m_1)/c_3) \\ k_3 &= m_0 / c_3 \end{aligned} \tag{11}$$

The BD diagram of the fractional high-pass filters of order $(1+\alpha)$ is portrayed in Fig.2. The transfer function of this topology is given by

$$H(s) = \frac{G_3 s^3 + \dfrac{G_2}{T_1}s^2 + \dfrac{G_1}{T_1 T_2}s}{s^3 + \dfrac{1}{T_1}s^2 + \dfrac{1}{T_1 T_2}s + \dfrac{1}{T_1 T_2 T_3}} \tag{12}$$

By equating (10) with (12), it can be found that

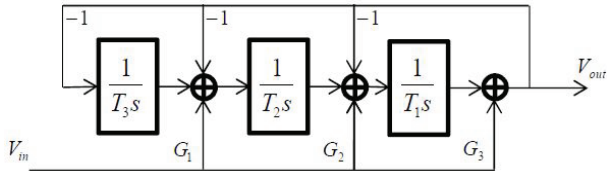$$G_3 = \frac{c_1 m_0}{c_3 k_0}, G_2 = \frac{c_1 m_1}{c_3 k_1}, G_1 = \frac{c_1 m_2}{c_3 k_2}$$

$$T_1 = \frac{k_0}{k_1}, T_2 = \frac{k_1}{k_2}, T_3 = \frac{k_2}{k_3}$$

(13)

Figure 2: The BD diagram of the approximated Butterworth high-pass fractional order filter

2.3 Fractional low-pass filters of order (n+α)

The transfer functions of the fractional low-pass filters of order (n+α) could be reached by using polynomial division given by (14) [3]

$$H_{n+\alpha}^{FLPF}(s) = \frac{H_{1+\alpha}^{FLPF}(s)}{B_{n-1}^{LP}(s)}$$

(14)

where $H_{1+\alpha}^{FLPF}(s)$ is the fractional low-pass filter given by (5) and $B_{n-1}^{LP}(s)$ is the (n−1) order standard low-pass Butterworth polynomial.

From (14), the general form of fractional low-pass filters is derived as

$$H_{n+\alpha}^{FLPF}(s) \cong \frac{X_2 s^2 + X_1 s + X_0}{Y_{n+2} s^{n+2} + Y_{n+1} s^{n+1} + ... + Y_1 s + Y_0}$$

(15)

where the coefficients X_i (i=0,1,2) and Y_i (i=n+2, n+1,...0) can be found using k_j and m_j (j=0,1,2) in (5) and the coefficients of the Butterworth low-pass polynomial $B_{n-1}^{LP}(s)$.

The BD diagram of the fractional low-pass filters of order (n+α) is shown in Fig.3b. The transfer function of this topology is expressed as

$$H_{n+\alpha}^{FLPF}(s) = \frac{\dfrac{G_2}{T_1 T_2 ... T_n} s^2 + \dfrac{G_1}{T_1 T_2 ... T_{n+1}} s + \dfrac{G_0}{T_1 T_2 ... T_{n+2}}}{s^{n+2} + \dfrac{1}{T_1} s^{n+1} + \dfrac{1}{T_1 T_2} s^n + ... + \dfrac{1}{T_1 T_2 ... T_{n+2}}}$$

(16)

By equating (15) with (16), it can be obtained that

$$G_i = \frac{X_i}{Y_i}, i = 0,1,2$$

$$T_i = \frac{Y_j}{Y_{j-1}}, i = 1,2,...,n+2; j = n+2,...,1$$

(17)

An alternative way of the realization of the fractional low-pass filters of (n+a) is the cascade connection of fractional order filter $H_{1+a}^{FLPF}(s)$ and Butterworth filter of order (n−1) as portrayed in Fig.3a. The transfer function of the block is given as [23]

$$H_{n+\alpha}^{FLPF}(s) = H_{1+\alpha}^{FLPF}(s) \frac{1}{B_{n-1}^{LP}(s)}$$

(18)

where $B_{n-1}^{LP}(s)$ is the (n−1) order low-pass Butterworth polynomial.

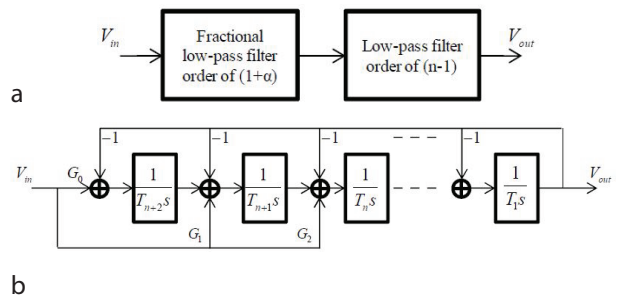**Figure 3:** The realization of the approximated Butterworth low-pass fractional (n+a) order filters via: a cascade connection; b polynomial division

2.4 Fractional high-pass filters of order (n+α)

As following the similar procedure carried out in the section of the (n+α) order fractional low-pass filters, the developed BD diagram and design equations for their high-pass counterparts are depicted in Fig.4 and expressed as

$$H_{n+\alpha}^{FHPF}(s) = \frac{H_{1+\alpha}^{FHPF}(s)}{B_{n-1}^{HP}(s)}$$

(19)

where $H_{1+a}^{FHPF}(s)$ is the fractional high-pass filter given by (10) and $B_{n-1}^{HP}(s)$ is the Butterworth high-pass polynomial derived by writing 1/s instead of s in $B_{n-1}^{LP}(s)$. Substituting (10) into (19), the general IFLF form of fractional high-pass filters is obtained as

$$H_{n+\alpha}^{FHPF}(s) \cong \frac{X_3 s^2 + X_2 s + X_1}{Y_{n+2} s^{n+2} + Y_{n+1} s^{n+1} + ... + Y_1 s + Y_0}$$

(20)

where the coefficients X_i (i=1,2,3) and Y_i (i=n+2, n+1,...0) can be derived using k_j (j=0,1,2,3) in (11) and m_j (j=0,1,2)

in (6) and the coefficients of the Butterworth high-pass polynomial $B^{HP}_{n-1}(s)$.

From Fig.4b, the transfer function of this topology is found as

$$H^{FHPF}_{n+\alpha}(s) = \frac{G_3 s^{n+2} + \dfrac{G_2}{T_1} s^{n+1} + \dfrac{G_1}{T_1 T_2} s^n}{s^{n+2} + \dfrac{1}{T_1} s^{n+1} + \dfrac{1}{T_1 T_2} s^n + ... + \dfrac{1}{T_1 T_2 ... T_{n+2}}} \quad (21)$$

By equating (20) with (21), it can be obtained that

$$G_i = \frac{X_i}{Y_j}, i = 1,2,3; \ j = n, n+1, n+2$$

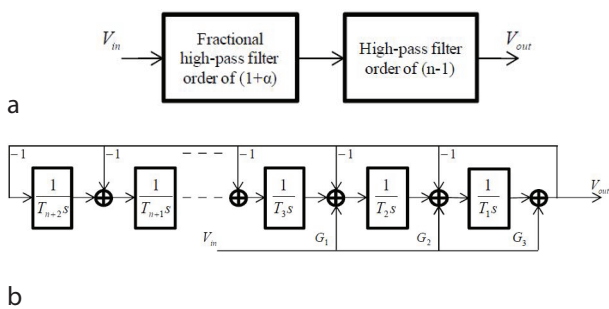$$T_i = \frac{Y_j}{Y_{j-1}}, i = 1,2,...,n+2; \ j = n+2,...,1 \quad (22)$$

a

b

Figure 4: The realization of the approximated Butterworth high-pass fractional (n+α) order filters via: a cascade connection; b polynomial division

The transfer function of the Fig.4a is given by

$$H^{FHPF}_{n+\alpha}(s) = H^{FHPF}_{1+\alpha}(s) \frac{1}{B^{HP}_{n-1}(s)} \quad (23)$$

where $B^{HP}_{n-1}(s)$ is the (n−1) order high-pass Butterworth polynomial.

Band-pass filters can also be attained by cascading the high-pass and low-pass filters as demonstrated in Fig.5.
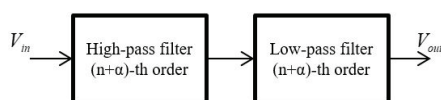

Figure 5: The realization of the approximated Butterworth band-pass fractional (n+α) order filters via cascade connection

3 OTA-C based realizations of the fractional filters

To achieve very low cut-off frequencies with OTA-C filters, very low transconductance values are required. In order to achieve low transconductance values, the OTA structure shown in Fig.6 is chosen [26]. It is chosen due the fact that this OTA building block has very simple internal construction to provide advantages of less power consumption and chip area. At the same time, it allows a wide range of transconductance controllability. Moreover, its linear input range is improved over the classical differential pair. In this scheme, the input voltages V_{ip} and V_{in} are applied to improved cross coupled MOS (Metal Oxide Semiconductor) cell composed of M_1-M_2 and M_3-M_4. The output current I_0 is related to input differential voltage (V_{ip}–V_{in}) as $I_0=g_m \times (V_{ip}$–$V_{in})$. The OTA is biased in manner of operating in subthreshold region for low voltage operation. The transconductance of the OTA is adjusted by the bias current source I_B. The supply voltages V_{DD} and V_{CC} are selected as +0.75 V and −0.75 V, respectively. The output current expression of the chosen OTA is given by

$$I_o = I_B \left(\tanh(\frac{V_{id}}{2nV_T} + \frac{\ln m}{2}) + \tanh(\frac{V_{id}}{2nV_T} - \frac{\ln m}{2}) \right) \quad (24)$$

where the V_{id} is the input voltage difference (V_{ip}–V_{in}), V_T is the thermal voltage, m is the ratio of aspect ratios of the $M_1(M_2)$ and $M_3(M_4)$ and n is the subthreshold slope factor.
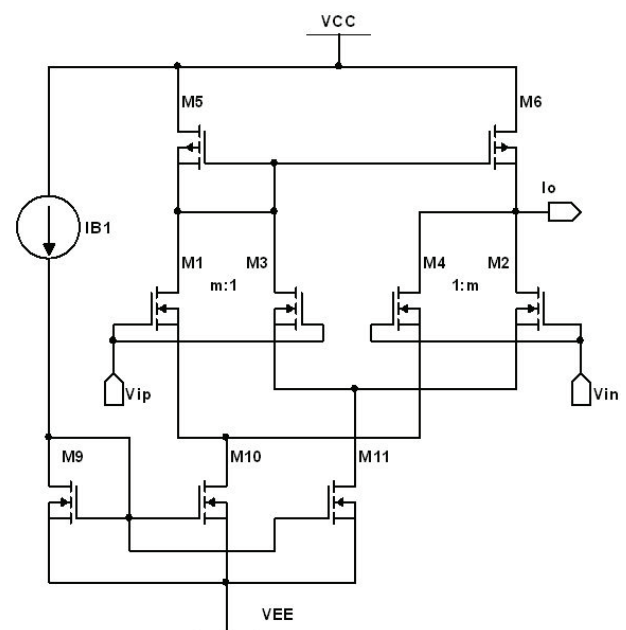

Figure 6: The used OTA structure

The realized filter topologies are depicted in Fig.7 and Fig.8, respectively. From these figures, the related time constants could be expressed as

$$T_k = \frac{C_k}{g_{mk}} \tag{25}$$
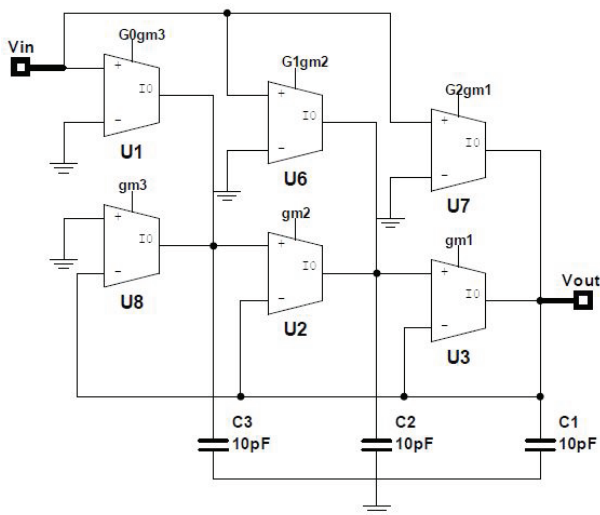
where k is 1, 2 and 3.

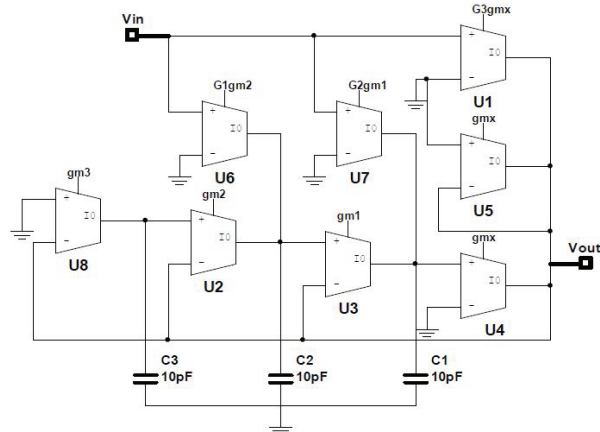**Figure 7:** The circuit of OTA-C based fractional order Butterworth low-pass filter of order (1+α)

Figure 8: The circuit of OTA-C based fractional order Butterworth high-pass filter of order (1+α)

Adding extra (n−1) OTA-C integrators to Fig.7 and Fig.8, the (n+α) order low-pass and high-pass filters are realized according to the polynomial division method, respectively. If the cascade connection method is preferred, the circuit of the (n−1) order corresponding Butterworth filters should be connected to output ports of circuits in Fig.7 and Fig.8, respectively.

4 Simulation

In this section, while the circuit level simulations of the OTA-C based low-pass and high-pass filters of order (n+α) are performed via PSPICE with 0.35 μm TSMC CMOS technology parameters, their corresponding transfer functions are simulated numerically. Then both of the results are given in comparative way.

4.1 The Approximated fractional Butterworth low-pass filters

The parameters given by (9) are calculated and the scaled versions according to f = 100Hz are given in Table 1 for α = 0.3 and α = 0.5.

Table 1: The calculated parameters given by (9) for α = 0.3 and α = 0.5

	α = 0.3	α = 0.5
T_1	$4.6\ 10^{-4}$	$5.5\ 10^{-4}$
T_2	$14\ 10^{-4}$	$14\ 10^{-4}$
T_3	$61\ 10^{-4}$	$54\ 10^{-4}$
G_0	1.01	1.01
G_1	0.685	0.6
G_2	0.115	0.07

From Table 1, the required bias currents of OTAs for α = 0.5 and for α = 0.3 with the equal values of the integrator capacitors of 10 pF are calculated and given in Table 2.

Table 2: The calculated bias current of OTAs according to Table 1

	α = 0.3	α = 0.5
I_{b1}	1.8 nA	1.5 nA
I_{b2}	573 pA	597 pA
I_{b3}	135 pA	154 pA

The results of frequency simulations for α = 0.5 and α = 0.3 are demonstrated in Fig.9, the corresponding theoretical values are also given in same figure. It can be clearly seen from the Fig.9 that the stop-band attenuation changes according to the fractional order α which supports the theoretical statements, as it is expected. The derived stop-band attenuations for α = 0.5 and α = 0.3 are respectively −30.4 dB/dec and −25.61 dB/dec in the range of 628 to 6280 rad/sec, which are close to −20×(1.5) dB/dec = −30 dB/dec and −20×(1.3) dB/dec = −26 dB/dec. Therefore, unlike the integer order filters, stop-band attenuation of −20×(α+1) dB/dec can be achieved closely. Moreover, the stop-band attenuation increases by increasing the order α. However, it should

be taken into account that there is not a very precise slope of attenuation beyond 6280 rad/sec because the used approximation function is just the second order form. On the other hand, the filter presents quite flat response in the pass-band for the all values of α.
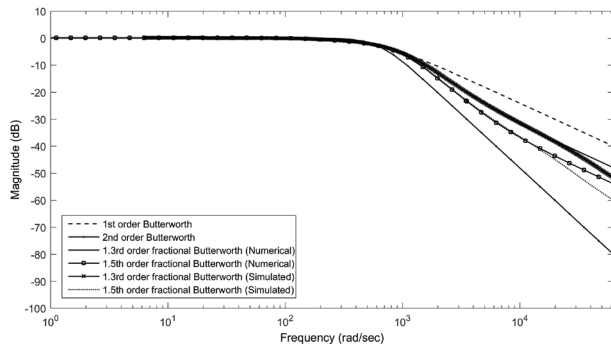

Figure 9: The numerical and simulated responses of fractional Butterworth low-pass filters of different orders

The power dissipations of low-pass filters of orders 1.3 and 1.5 are derived as 14.6 nW and 13 nW, respectively. Hence, the proposed filter topologies are suitable for low power applications.

In order to compare proposed filter circuits with the others in the literature, some performance parameters are given in Table 3. It can be deduced from Table 3 that proposed circuits outperform the work in [23] in terms of power efficiency as well as slope of stop-band attenuation. Additionally, proposed filters support electronic tuning in contrast to the work in [23]. On the other hand, even though the work in [22] has advantages over proposed circuits in terms of power consumption and supply voltage, it needs very low and accurate bias currents so it can be very difficult to achieve such a very low and accurate current levels. Different from works of [22-23], comparing proposed circuits with the others, proposed filters have advantages of the low power consumption and low supply voltage, integration capability, good slope of the stop-band attenuation and electronic tunability. But it should be considered that other circuits except the works of [22-23] are based on discrete form circuit components.

To observe output Total Harmonic Distortion (THD) level, a fixed frequency of 30 Hz and variable amplitude sinusoidal input signal is applied to the fractional low-pass filters. The realized output is presented in Fig.10.

Table 3: The comparison of some performance parameters of the fractional order filters of order 1.5

		[3]	[14]	[16]	[18]	[22]	[23]	This study
Filter Types		LP-HP	LP-HP BP -BR	LP-HP BP	LP	LP-HP	LP	LP-HP
Approx. Method - order		CFE -2nd	CFE -4th	CFE -2nd	FEA	CFE -2nd	CFE -2nd	CFE -2nd
Circuit configuration		FPAA based	RLC circuit	SAB circuit	CCII based	Sinh/Log domain building block based	DDCC based	OTA based
Mode		VM	VM	VM	VM	CM	VM	VM
Technology		-	-	-	-	0.18 μm	0.35 μm	0.35 μm
Voltage supply		-	-	-	-	500 mV	±500 mV	±750mV
Electronic tunability		Supported	Not supported	Not supported	Not supported	Supported	Not supported	Supported
Integration capacitor (min)		-	-	-	-	60 pF	751 pF	10 pF
Power cons. (Sim.)	LP					5.47 nW	185 μW	13 nW
	HP	-	-	-	-	3.56 nW	-	42.7 nW
Cut-off freq. (Theo.\Sim..)	LP	1 kHz \ -	1 kHz \ -	- \ -	- \160 Hz	10 Hz \11.8 Hz	1.7 kHz \-	100 Hz \101.6 Hz
	HP	10 kHz \ -	- \ -	- \ -	- \ -	- \3.87 Hz	- \ -	100 Hz \100.3 Hz
Stop-band attenuations Sim. (Theoretically -30 dB/ dec or -6 dB/oct)	LP	-30.75 dB/ dec	-	-29.74 dB/dec	-	-9.1 dB/oct	-31 dB/dec	- 30.4 dB/dec
	HP	-29.49 dB/ dec	-	-	-	-9.2 dB/oct	-	-29.7 dB/dec

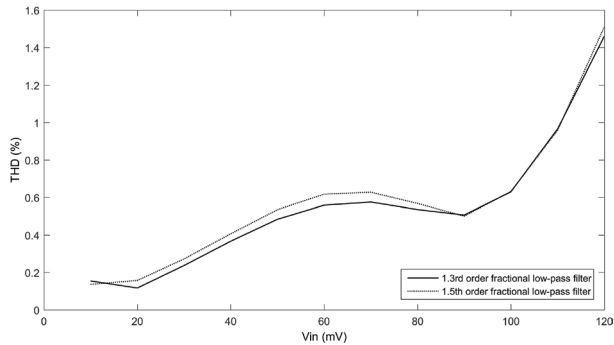It is clearly seen that, the THD level is acceptable up to 120 mV input amplitude.

Figure 10: The output THD versus a fixed frequency-variable amplitude input voltage

To evaluate the time domain response of the low-pass filter, as an input, a 30 Hz sinusoidal signal with 50 mV amplitude is applied to filter of order $\alpha = 0.5$. The obtained output signal is shown in Fig.11.
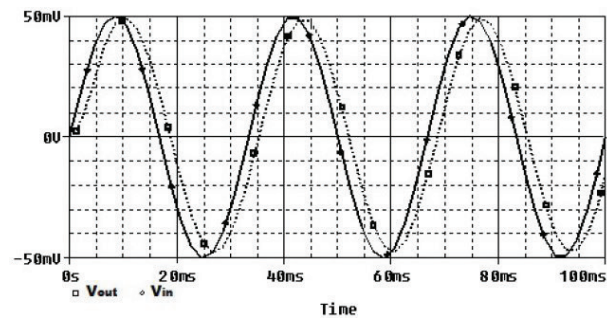

Figure 11: The time domain response of the 1.5th order fractional Butterworth low-pass filter

To gain more insights about higher order fractional filters and show applicability of the cascade realization, the simulated responses of the 2.3rd and 2.5th order fractional low-pass filters are depicted in Fig.12. The power dissipations of low-pass filters of orders 2.3 and 2.5 are derived as 17 nW and 15.3 nW, respectively. The simulated pass-band attenuations of these filters are respectively −45.3 dB/dec and −50.13 dB/dec while their theoretical values are −45 dB/dec and −50 dB/dec.

4.2 The Approximated fractional Butterworth high-pass filters

The parameters provided by (13) are calculated and given in Table 4 for $\alpha = 0.3$ and $\alpha = 0.5$, respectively.
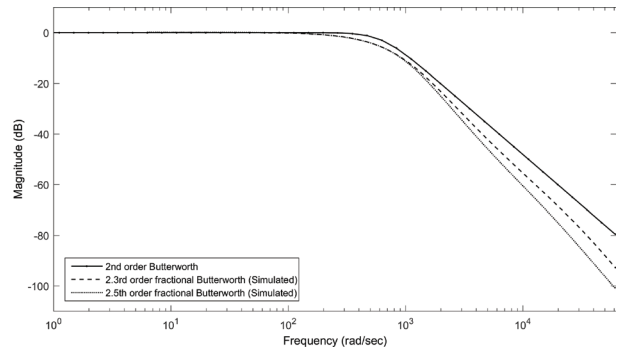

Figure 12: The simulated responses of the 2.3rd and 2.5th order fractional Butterworth low-pass filters

Table 4: The calculated parameters given by (13) for $\alpha = 0.3$ and $\alpha = 0.5$

	$\alpha = 0.3$	$\alpha = 0.5$
T_1	4.13×10^{-4}	4.71×10^{-4}
T_2	18×10^{-4}	18×10^{-4}
T_3	55×10^{-4}	46×10^{-4}
G_1	0.12	0.07
G_2	0.68	0.6
G_3	1	1

According to Table 4, the corresponding bias currents of OTAs for $\alpha = 0.5$ with the same values of the capacitors of 10 pF are obtained and presented in Table 5.

The results of simulations for $\alpha = 0.3$ and $\alpha = 0.5$ are illustrated in Fig.13. It can be deduced from the Fig.13 that the stop-band attenuation changes according to fractional order α. The reached stop-band attenuations for $\alpha = 0.5$ and $\alpha = 0.3$ are respectively −29.7 dB/dec and −25.5 dB/dec, which are close to $-20 \times (1.5)$ dB/dec = −30 dB/dec and $-20 \times (1.3)$ dB/dec = − 26 dB/dec.

Table 5: The calculated bias current of OTAs according to Table 4

	$\alpha = 0.3$	$\alpha = 0.5$
I_{b1}	2 nA	1.75nA
I_{b2}	467 pA	448 pA
I_{b3}	149 pA	178 pA
I_{bx}	2 nA	2 nA

The power consumptions of high-pass filters of orders 1.3 and 1.5 are simulated as 45.2 nW and 42.7 nW, respectively. The main reason of higher power dissipations of the high-pass filters in contrast to their low-pass counterparts is the summation node constructed by the U4(g_{mx}) and U5($1/g_{mx}$) shown in Fig.8.
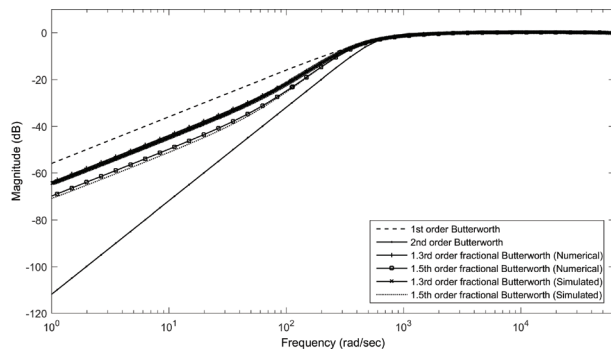
Figure 13: The numerical and simulated responses of fractional Butterworth high-pass filters of different orders

To evaluate output THD level versus input voltage, a fixed frequency of 1 kHz and variable input sinus is applied to the fractional high-pass filters. The obtained THD level doesn't exceed 2.9% up to 120 mV input voltage. Thus, the high-pass filters can be kept in acceptable THD range up to 120 mV input amplitude.

To attain higher order fractional high-pass filters, the cascade connection is preferred because of its simplicity. The simulated responses of the 2.3rd and 2.5th order fractional high-pass filters are presented in Fig.14. The power dissipations of high-pass filters of orders 2.3 and 2.5 are derived as 47.5 nW and 45 nW, respectively. The simulated pass-band attenuations of these filters are respectively –45.1 dB/dec and –49.3 dB/dec while their theoretical values are –46 dB/dec and –50 dB/dec.
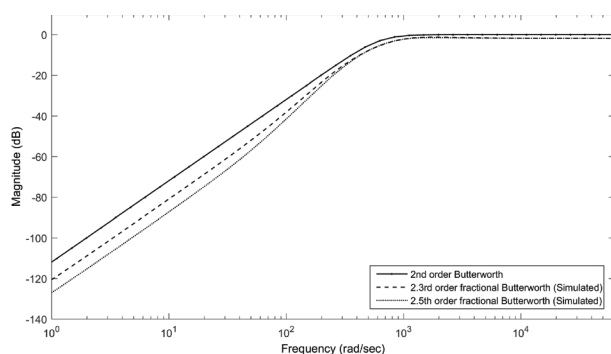

Figure 14: The simulated responses of the 2.3rd and 2.5th order fractional Butterworth high-pass filters

5. Conclusion

In this study, the OTA-C based approximated fractional order Butterworth filters are introduced, designed and simulated. The general design equations are derived and given in order for the readers. Even though the fractional filters are approximated by higher degree integer order transfer functions or R-C networks com-

posed of the many branches, these are the simple ways of circuit implementations until fractional electronic components become commercially available. The simulation results confirm theoretical statements. However, it should be taken into account that there are small deviations from the ideal cases due to approximation functions, rounding errors and the non-ideal characteristics of active elements. Nevertheless, it can be said that unlike their integer order counterparts, fractional order filters provide fractional stepping attenuation in the stop-band. Furthermore, it can be deduced from simulations that the proposed filter topology is appropriate for low amplitude-low frequency signals like biomedical signals, such as EEG (electroencephalograph), EOG (electrooculogram). This is because the frequency bandwidth of the filters is not very wide owing to the approximation functions used. At the same time, since the proposed fractional filter topologies allow for attenuation of less than multiples of 20 dB/dec, more information could be kept in the stop-band in comparison with their integer order counterparts. In addition, the proposed filter circuits allow for electronic tuning of order and frequency response without any structural changes on related topologies and also provide the low-voltage low-power operation.

6 References

1. Ortigueira, M. D: 'An introduction to the fractional continuous time linear systems: the 21st century systems', IEEE Circuits and Systems Magazine, 2008, 8, (3), pp. 19-26
2. Elwakil, A. S.: 'Fractional-order circuits and systems: emerging interdisciplinary research area', IEEE Circuits and Systems Magazine, 2010, 10, (4), pp. 40-50
3. Freeborn, T. J., Maundy, B., Elwakil, A. S.: 'Field programmable analogue array implementation of fractional step filters', IET Circuits, Devices and Systems, 2010, 4, (6), pp. 514-524
4. Radwan, A. G., Elwakil, A. S., Soliman, A. M.: 'Fractional-order sinusoidal oscillators: design procedure and practical examples', IEEE Transactions on Circuits and Systems-1, 2008, 55, (7), pp. 2051-2063
5. Maundy, B., Elwakil, A., Gift, S.: 'On a multivibrator that employs a fractional capacitor', Analog Integrated Circuits and Signal Processing, 2010, 62, pp. 99-103
6. Tripathy, M. C., Mandal, D., Biswas, K., et al.: 'Design and performance study of phase locked-loop using fractional order loop filter', International Journal of Circuit Theory and Applications, 2014, 43, (6), pp. 776-792

7. Podlubny, I., Petras, I., Vinagre, B. M., *et al.*: 'Analogue realizations of fractional-order controllers', Nonlinear Dynamics, 2002, 29, (1), pp. 281-296

8. Bohannan, G. W.: 'Analog fractional order controller in temperature', Journal of Vibration and Control, 2008, 14, (9-10), pp. 1487-1498

9. Krishna, B. T.: 'Studies on fractional order differentiators and integrators: a survey', Signal Processing, 2011, 91, (3), pp. 386-426

10. Santamaria, G., Valuerde, J., Perez-Aloe, R., *et al.*: 'Microelectronic implementations of fractional order integrodifferential operators', Journal of Computational and Nonlinear Dynamics, 2008, 3, (2).

11. Varshney, P., Gupta, M., Visweswaran, G. S.: 'Implementation of switched capacitor fractional order-differentiator (PD$^\delta$) circuit', International Journal of Electronics,2008, 95, (6), pp. 1105-1126

12. Acharya, A., Das, S., Pan, I., *et al.*: 'Extending the concept of analog Butterworth filter for fractional order systems', Signal Processing, 2014, 94, pp. 409-420

13. Radwan, A. G., Elwakil, A. S., Soliman, A. M.: 'On the generalization of second order filters to the fractional order domain', Journal of Circuits, Systems and Computers, 2009, 18, (2), pp. 361-386

14. Freeborn, T. J., Maundy, B., Elwakil, A.: 'Fractional resonance based RLβCα filters', Mathematical Problems in Engineering, 2013, (2013)

15. Soltan, A., Radwan, A. G., Soliman, A. M.: 'Butterworth passive filter in the fractional order', International Conference on Microelectronics, Hammamet, 2011, pp. 1-5

16. Maundy, B., Elwakil, A. S., Freeborn, T. J.: 'On the practical realization of higher-order filters with fractional stepping', Signal Processing, 2011, 91, (3), pp. 484-491

17. Radwan, A., Soliman, A., Elwakil, A.: 'First order filters generalized to the fractional domain', Journal of Circuits, Systems and Computers, 2008, 17, (1), pp. 55-66

18. Soltan, A., Radwan, A. G. &Soliman, A. M.: 'CCII based fractional filters of different orders', Journal of Advanced Research, 2014, 5, (2), pp. 157-164

19. Freeborn, T., Maundy, B., Elwakil, A. S.: 'Approximated fractional order Chebyshev lowpass filters', Mathematical Problems in Engineering, 2014, (2014)

20. Tripathy, M. C., Biswas, K., Sen, S.: 'A design example of a fractional order Kerwin-Huelsman-Newcomb biquad filter with two fractional capacitors of different order', Circuits, Systems, and Signal Processing, 2013, 32, (4), pp. 1523-1536

21. Tripathy, M. C., Mandal, D., Biswas, K., *et al.*: 'Experimental studies on realization of fractional inductors and fractional order bandpass filters', International Journal of Circuit Theory and Applications, 2014, 43, (9), pp. 1183-1196

22. Tsirimokou, G., Laoudias, C., Psychalinos, C.: '0.5-V fractional order companding filters', International Journal of Circuit Theory and Applications, 2014, 43, (9), pp. 1105-1126

23. Khateb, F., Kubanek, D., Tsirimokou, G., *et al.*: 'Fractional order filters based on low voltage DDCCs', Microelectronics Journal, 2016, 50, pp. 50-59

24. Das., P., Pan, I.: 'Basics of fractional order signals and systems', 'Fractional Order Signal Processing: Introductory Concepts and Applications' (Springer Press, 2012), pp. 13-30

25. Radwan, A. G., Soliman, A. M., Elwakil, A. S. et al.: 'On the stability of linear systems with fractional order elements', Chaos, Solitans and Fractals, 2009, 40, (5), 2317-2328

26. 'Transconductors in subthreshold CMOS', http://wordpress.nmsu.edu/pfurth/files/2015/06/cissd1995.pdf, accessed 22 November 2016